ISSN 1054-660X, Laser Physics, 2011, Vol. 21, No. 4, pp. 774–781.

$GaS_{0.4}Se_{0.6}$: Relevant Properties and Potential for 1064 nm Pumped Mid-IR OPOs and OPGs Operating above 5 μm[1]

V. Petrov[a, *], V. L. Panyutin[a], A. Tyazhev[a], G. Marchev[a], A. I. Zagumennyi[b], F. Rotermund[a, c], F. Noack[a], K. Miyata[a], L. D. Iskhakova[b], and A. F. Zerrouk[d]

[a] *Max-Born-Institute for Nonlinear Optics and Ultrafast Spectroscopy, 2A Max-Born-Str., D-12489 Berlin, Germany*

[b] *General Physics Institute of the Russian Academy of Sciences, ul. Vavilova 38, Moscow, 117942 Russia*

[c] *Division of Energy Systems Research, Ajou University, San 5 Wonchun-dong, 443-749 Suwon, Republic of Korea*

[d] *Zecotek Photonics Singapore Pte Ltd., 20 Science Park Rd, no. 01-23/25, Teletech Park, Science Park II, 117674 Singapore*

*e-mail: petrov@mbi-berlin.de

Received April 22, 2010; in final form June 2, 2010; published online March 4, 2011

Abstract—We present measurements of the transparency, refractive index dispersion, nonlinear coefficient, damage threshold, and two-photon absorption of mixed GaS_xSe_{1-x} crystals and show that $GaS_{0.4}Se_{0.6}$ is a promising nonlinear material for down conversion of pulsed 1064 nm radiation to the mid-IR above 5 μm without significant two-photon absorption.

DOI: 10.1134/S1054660X11070255

1. INTRODUCTION

The nonlinear optical properties of mixed GaS_xSe_{1-x} crystals with $x = 0.2$ and 0.4 were studied as early as 1982 [1]. A Q-switched CO_2 laser operating at 130 Hz, with a peak power of ~400 W, was used for second-harmonic generation (SHG) and relative measurements of the efficiency led to $d_{22}(x = 0.2) = (0.525 \pm 0.05)d_{22}(\text{GaSe})$ and $d_{22}(x = 0.4) = (0.31 \pm 0.05)d_{22}(\text{GaSe})$ for the nonlinear coefficients. In addition, the authors of [1] demonstrated difference-frequency generation from 7 to 12.5 μm with $GaS_{0.2}Se_{0.8}$. Index of refraction was measured and Sellmeier equations were fitted for $x = 0$, 0.2, 0.4, 0.8, and 1.0 in the range 0.63 μm $< \lambda <$ 20 μm. The observed strong reduction of the nonlinear coupling constant with increasing S content and deterioration of the crystal quality in comparison to the two parent compounds, GaS and GaSe obviously contributed to the lacking interest in further investigation of such solid solutions. A phase transition from the non-centrosymmetric (ε) phase of GaSe, corresponding to the $\bar{6}m2$ point group, to a centrosymmetric (β) phase, corresponding to the $6/mmm$ point group, is indicated in [1] for $0.2 < x < 0.3$. The limits of the possible polytypes occurring in the GaS_xSe_{1-x} solid solutions were given more systematically in [2] as:

ε for $x = 0$ (GaSe) to $x \approx 0.01$

ε–γ mixture for x between ≈0.01 and ≈0.03

γ for x between ≈0.05 and ≈0.4

β for x from ≈0.5 to 1 (GaS).

Above, the γ phase corresponds to the non-centrosymmetric point group 3m. These results were confirmed in the more recent work [3] where the mixed phase ε–γ is associated with $0 \le x \le 0.4$, a mixture of ε–γ and β was observed for $x = 0.5$ and pure β phase for GaS, see [4] for an overview. However, the question about the transitions between the phases is very complex and has not found a satisfactory solution, yet. Four phases are identified for GaSe itself in the literature while GaS crystallizes only in the β-phase. The literature on GaS_xSe_{1-x} compounds is often controversial concerning this issue and it seems that there is some dependence on the growth conditions [5, 6]. Recently the phase-matching properties of a series of solid solutions with x ranging from 0.04 to 0.412 were measured for SHG of 2.79 μm (Er : YSGG laser) and 9.56/9.58 μm (CO_2 laser) radiation [7, 8]. The phase-matching angle varied only little with the composition but these authors speculated that the conversion efficiency with $GaS_{0.09}Se_{0.91}$ is 2.4 times higher than that of pure GaSe [8] and approximately so much higher in comparison to In-doped GaSe [7]. Both results are rather unexpected since they contradict the general trends observed as a function of the band-gap, which grows with S-content but decreases with In-content [9], as well as the conclusions in [1], thus a direct evaluation of the nonlinear coefficients of GaS_xSe_{1-x} crystals is desirable.

[1] The article is published in the original.

Table 1. Average composition and compositions with extreme content of components

Ga	S	Se	Δ, at. %
1.008	0.407	0.585	0
0.978(min)	0.438(max)	0.584	3.7
1.021(max)	0.404	0.575(min)	1.3
1.010	0.391(min)	0.599(max)	2.2

Two essential advantages can be expected from adding S to the well known nonlinear crystal GaSe: increase of the band-gap value or the short wave cut-off limit [10, 11] and increased hardness [12] which is one of the basic limitations of GaSe. A microhardness of ~40 kgf/mm^2 (2.9–3.0 in the Mori's scale) can be found in [12] for a composition of $GaS_{0.4}Se_{0.6}$. Stronger dependence on the composition and an increase from 7–8 to 15 kgf/mm^2 with x from 0 to 0.09 has been reported in [13]. Note that while In-doping could also be useful for improvement of the opto-mechanical properties of GaSe, its distribution coefficient is low [14, 15] and such mixed crystals do not show extended transparency [13].

The present study focuses on measurements of the transmission, dispersion, nonlinear coefficient, damage threshold, and two-photon absorption (TPA) of GaS_xSe_{1-x} in the $0 \le x \le 0.4$ range. The motivation for this work is the expectation that around $x = 0.4$, a number of characteristics such as band-gap, transparency, effective nonlinearity, damage threshold, and microhardness will make this solid solution suitable for nanosecond/picosecond pumping of optical parametric oscillators (OPO) or optical parametric generators/amplifiers (OPG/OPA) at 1064 nm (Nd : YAG laser systems) without the onset of TPA. Note that TPA is an unwanted higher-order nonlinear process, which can be avoided at 1064 nm only in very few chalcogenide compounds, most of them with modest nonlinearity [16]. For operation at higher repetition rates, the thermal conductivity is another property that has to be taken into account. According to [17], the thermal conductivity of GaSe and GaS are rather high (~11 and ~9 W/mK, respectively) parallel to the plane of the crystal layers. Although the conductivity along the crystal axis is 6 to 9 times lower, this seems not to be a serious disadvantage, because phase-matching in these crystals, due to the large birefringence, is often confined to small internal angles with respect to the c-axis and thermal lensing will be suppressed. However, one cannot rule out the possibility that solid solutions in the GaS–GaSe system exhibit lower conductivity than the two parent compounds [18].

2. CRYSTAL GROWTH AND COMPOSITION

GaS_xSe_{1-x} crystals were grown for compositions $x = 0$, 0.05, 0.10, 0.40 in the charge. The elemental purity was Ga(99.9999%), Se(99.999%) and S(99.999%). The measured melting temperatures for these compounds were (960 ± 10)°C. Single crystals were grown by the Bridgman–Stockbarger method in quartz ampoules with a diameter of 14 mm. The crystallization front velocity was 3 mm/day and the whole growth process took 20–25 days. Uniform single crystals up to 60 mm in length were grown, see Fig. 1. Interestingly, it was observed that for the composition with $x = 0.4$ the crystals grow without any "cap" at the top of the boule. This means that the charge and crystal compositions are identical. This observation could possibly mean congruent melting character, which is equivalent to the existence of a separate compound in the system of solid solutions, and deserves further investigation.

The composition of the crystals grown was studied by electron microanalysis using INCA energy analytical system (Oxford Instruments) attached to a scanning electron microscope (JEOL JSM-5910LV). Plates of GaSe and $GaS_{0.4}Se_{0.6}$ were used for this purpose, which were cleaved from the central parts of the boules. Six points spread over an area of 1.5 cm^2 were tested for GaSe and eight points spreads over an area of 2 cm^2 were tested in $GaS_{0.4}Se_{0.6}$.

The average composition of GaSe was found to correspond to the chemical formula $Ga_{1.015}Se_{0.985}$. The composition with minimum Ga content corresponded to the stoichiometric one, GaSe, whereas the composition with maximum Ga content had a chemical formula of $Ga_{1.033}Se_{0.967}$. These results deviate substantially from the observations in [6] where a typical crystal composition of say $Ga_{0.92}Se_{1.08}$ means much larger and opposite in sign deviation from stoichiometry.

The average composition determined for $x = 0.4$ was $Ga_{1.008}S_{0.407}Se_{0.585}$. The excess of Ga indicates the same direction of deviation from stoichiometry as in GaSe but this deviation is twice smaller. The Se and S deviations are in opposite directions leading to an average cation–anion deviation of 0.8 at. %. The composition with minimum Ga content corresponds to the one with maximum S content and the chemical formula $Ga_{0.978}S_{0.438}Se_{0.584}$ whereas the composition with maximum Ga content corresponds to the one with minimum Se content and the chemical formula $Ga_{1.021}S_{0.404}Se_{0.575}$ (Table 1). The composition with minimum S content is $Ga_{1.010}S_{0.391}Se_{0.599}$, the same for which the Se content is maximized.

For the three components of $GaS_{0.4}Se_{0.6}$ it is useful to introduce average absolute deviations, these deviations Δ (in at. %) are included in Table 1. As could be expected, on the average (2.4 at. %), these deviations are larger than in GaSe (1.65 at. %). It is interesting to note that, according to Table 1, the maximum of the one component of $GaS_{0.4}Se_{0.6}$ corresponds to the minimum of another one while the third component is close to the average value in that case.

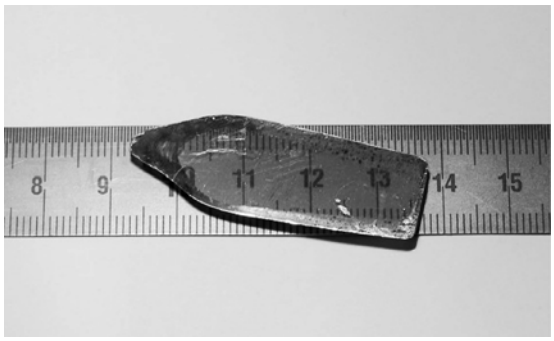

Fig. 1. Cleaved plate from an as grown crystal of $GaS_{0.4}Se_{0.6}$ with a thickness of 3.5 mm.

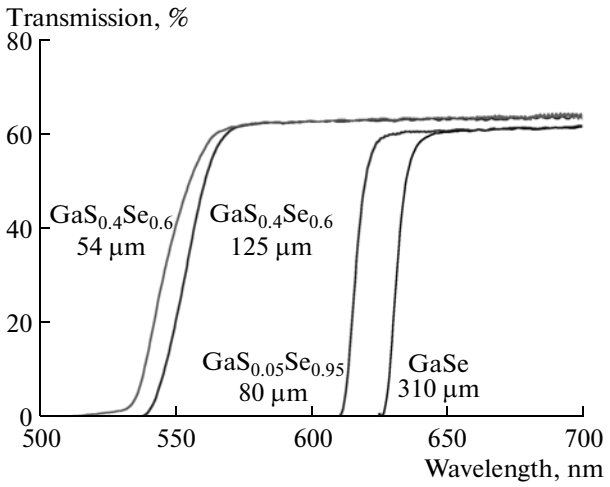

Fig. 2. Transmission of some GaS_xSe_{1-x} mixed crystals close to the band-gap (*o*-polarization).

3. BAND-GAP AND TRANSMISSION

For measurement of the visible absorption edge and estimation of the band-gap, thin plates with faces perpendicular to the *c*-axis and thickness between 50 and 600 μm were cleaved from the different crystals. Characteristic unpolarized spectra corresponding to the *o*-wave are shown in Fig. 2. They were used to compute the absorption coefficients $\alpha(h\nu)$ and $\alpha(\lambda)$ near the band-edge. The value of the direct band-gap was obtained from the linear fit to the $(\alpha h\nu)^2$ dependence on $h\nu$. There is good agreement with the results from [11] which are included in brackets in Table 2. It can be seen that the band-gap of $GaS_{0.4}Se_{0.6}$ corresponds to a wavelength very close to 532 nm which means that TPA will be greatly suppressed in this crystal for a pump wavelength of 1064 nm.

The full transmission spectrum was measured only for $x = 0$ and 0.4 using samples of 1.15 mm (GaSe) and 1.10 mm ($GaS_{0.4}Se_{0.6}$) thickness with the same orientation. The spectra were recorded on two spectrophotometers (visible/near-IR and Fourier transform) and the absolute values were calibrated (refined) by a laser measurement at 1564 nm. This measurement was performed by a highly stable diode-pumped femtosecond Er-fiber laser/amplifier to avoid interference effects from the two surfaces and the accuracy was better than 1%. Thus the calibrated transmission curves can be directly compared with the theoretical transmission, calculated by taking into account multiple reflections but neglecting the phase, which is also shown in Fig. 3 for both compounds.

It can be seen from Fig. 3 that both GaSe and $GaS_{0.4}Se_{0.6}$ have almost vanishing absorption losses in the regions of high transparency in the mid-IR. The 3 cm^{-1} transmission limits for the two crystals extend from 0.64 to 18 μm for GaSe and from 0.57 to 14.2 μm for $GaS_{0.4}Se_{0.6}$. As for GaSe, it is believed that the long wave transmission cut-off and also the absorption band of $GaS_{0.4}Se_{0.6}$ around 16 μm, which sets an upper wavelength limit for practical applications, are determined by multi-phonon processes. Like GaSe, $GaS_{0.4}Se_{0.6}$ also has an absorption feature before this band but it starts at shorter wavelengths, from about 10 μm, and the absorption at 10.6 μm amounts to 0.34 cm^{-1}, higher than in GaSe where it is 0.08 cm^{-1}. However, at 1064 nm $GaS_{0.4}Se_{0.6}$ exhibits about 5 times lower residual absorption (~0.12 cm^{-1} against ~0.6 cm^{-1}) than GaSe. This essential advantage comes from the fact that the absorption feature observed in GaSe in this wavelength range has disappeared in $GaS_{0.4}Se_{0.6}$. We note that this absorption feature has been present in most measurements of the GaSe transmission with sufficiently thick samples: from the earliest work [19] where the feature is well seen for a thickness of 1.5 and 6.0 mm, to more recent measurements [20, 21], where it transforms into an absorption arm for a thickness of 10 mm. Although absorption less than 0.25 cm^{-1} at 1064 nm has been reported for selected samples of GaSe [22], we are not aware of the physical mechanisms responsible for this residual absorption which seems to disappear in $GaS_{0.4}Se_{0.6}$.

Table 2. Room temperature band-gap parameters of GaSe and $GaS_{0.4}Se_{0.6}$, the data in brackets are from [11]

Composition	Sample thickness, μm	E_g, eV	λ_g, nm	$\alpha = 3$ cm^{-1} at λ, nm
$x = 0$	310	1.972(1.986)	629(625)	638
$x = 0.4$	125	2.278(2.276)	545(545)	569

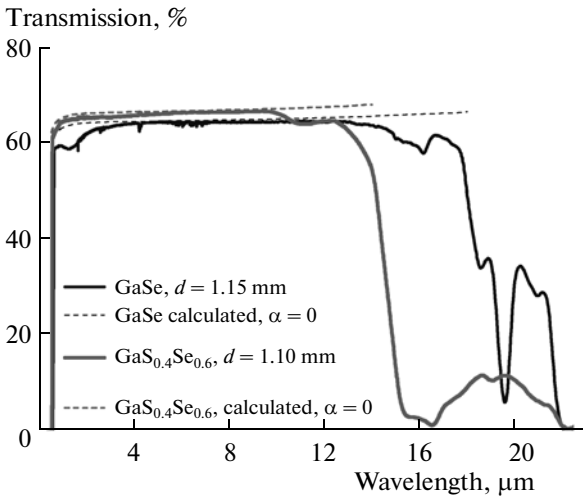

Fig. 3. Full measured transmission of GaSe and $GaS_{0.4}Se_{0.6}$ for *o*-polarization (thick lines), and theoretical calculation taking into account multiple reflections (thin lines).

4. DISPERSION AND BIREFRINGENCE

We measured the index of refraction of $GaS_{0.4}Se_{0.6}$ in the 0.633–10.0 μm spectral range using the autocollimation technique on a prism with aperture 15 × 15 mm and apex angle of 13.737°, shown in Fig. 4.

Table 3. Measured refractive indices and birefringence of $GaS_{0.4}Se_{0.6}$ at room temperature

λ, μm	n_o	n_e	$n_o - n_e$
0.6328	2.788	2.446	0.342
0.700	2.755	2.418	0.337
0.800	2.723	2.390	0.333
0.900	2.701	2.371	0.330
1.000	2.686	2.357	0.329
1.100	2.676	2.347	0.329
1.200	2.667	2.340	0.327
1.300	2.661	2.334	0.327
1.400	2.656	2.329	0.327
1.500	2.651	2.326	0.325
1.600	2.647	2.323	0.324
1.700	2.643	2.320	0.323
2.000	2.639	2.315	0.324
3.000	2.629	2.305	0.324
4.000	2.624	2.300	0.324
5.000	2.619	2.296	0.323
6.000	2.614	2.291	0.323
7.000	2.609	2.286	0.323
8.000	2.603	2.280	0.323
9.000	2.595	2.273	0.322
10.00	2.588	2.265	0.323

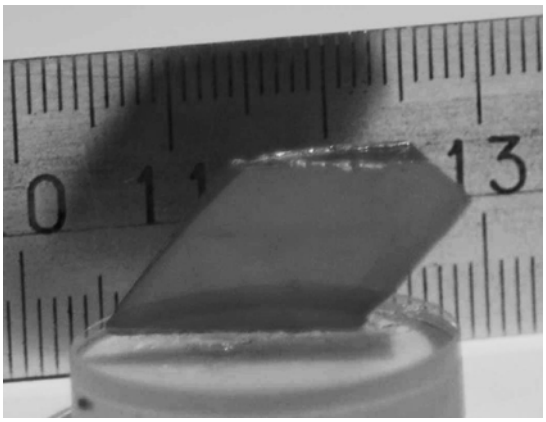

Fig. 4. Prism of $GaS_{0.4}Se_{0.6}$ used for measurement of the two refractive indices.

The two refractive indices measured and the birefringence are included in Table 3. From this data we fitted the following Sellmeier equations for $GaS_{0.4}Se_{0.6}$:

$$n_o^2 = 9.550489 + 0.303723/(\lambda^2 - 0.054331) + 3738.138/(\lambda^2 - 1408.38),$$

$$n_e^2 = 7.335355 + 0.247335/(\lambda^2 - 0.037580) + 2580.856/(\lambda^2 - 1268.56),$$

where the wavelength λ is in microns.

We did not try to refine the Sellmeier equations by using SHG phase-matching data since the accuracy of angle measurement far from normal incidence is limited [8]. Figure 5 shows a comparison of the predictions of the above Sellmeier equations for type-I (oo-e) SHG with experimental data. For completeness, similar curve and data are added for GaSe, with Sellmeier equations taken from [23]. The deviations in the case of $GaS_{0.4}Se_{0.6}$ are larger.

5. NONLINEAR COEFFICIENTS

The nonlinear coefficient of the mixed GaS_xSe_{1-x} compounds was measured by comparing the second harmonic conversion efficiency to that of pure GaSe. A $KNbO_3$-based femtosecond OPA was used as a laser source, operating at 4.65 μm at a repetition rate of 1 kHz, see Fig. 6. Direct generation of this wavelength is impossible starting from an ~800 nm, 45-fs Ti : sapphire regenerative amplifier system. Instead, a BBO type-II OPA was pumped near 800 nm and its idler output was frequency doubled in a BBO type-I crystal to provide a seed at the signal wavelength near 1 μm for the $KNbO_3$ crystal (6-mm, type-I, θ = 41.9°), which was also pumped near 800 nm by the same regenerative amplifier. The idler pulses of the $KNbO_3$ OPA were temporally broadened to about 350 fs but simultaneously spectrally narrowed (typical FWHM of

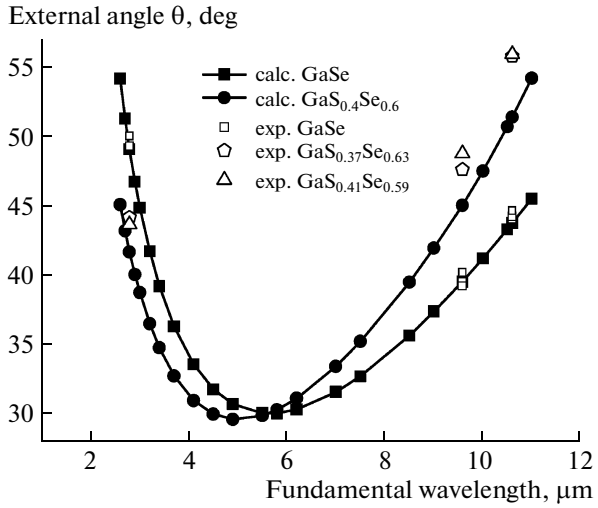

Fig. 5. SHG phase-matching in GaSe and GaS_xSe_{1-x}: calculation and experimental data from [8] (open symbols).

100 nm). The second harmonic generated in GaS_xSe_{1-x} crystals was detected by a pyroelectric energy meter after the fundamental had been suppressed by 2 cm of BK7 glass.

All GaS_xSe_{1-x} samples were cleaved with faces perpendicular to the *c*-axis and their thickness varied from 0.27 to 0.77 mm. Care was taken to have sufficient spectral and angular acceptance. For a fundamental energy of 3–4 μJ, the spot size was selected large enough so that spatial walk-off was negligible and the internal energy conversion efficiency remained below 10% (small signal approximation). The observed phase-matching angles for the different samples were very close and for calculation of the relative nonlinearities we only took into account the effect of the different index of refraction on the Fresnel losses and the coupling coefficient. For $x = 0$, 0.05, 0.1, and 0.4, two different samples of each kind were measured but the deviation for d_{22} was less than ±2%. For each sample the result was an average of 6 measurements rotating it about the *c*-axis (angle φ) with steps of 60° according to the symmetry ($d_{ooe} = d_{22}\cos\theta\sin 3\varphi$ for type-I phase-matching). Note that the second harmonic signal, scanned with a step of 2° in φ, dropped to zero between these angles which suggests that the symmetry of GaSe ($\bar{6}m2$ or ε phase as the main modification obtained from the melt [4]) is preserved or the *d*-coefficient which is independent of the azimuthal angle φ (in 3m symmetry or γ modification) has a negligible contribution. Thus, the results can be summarized as:

$$d_{22}(GaS_{0.05}Se_{0.95}) = 0.89\,d_{22}(GaSe),$$

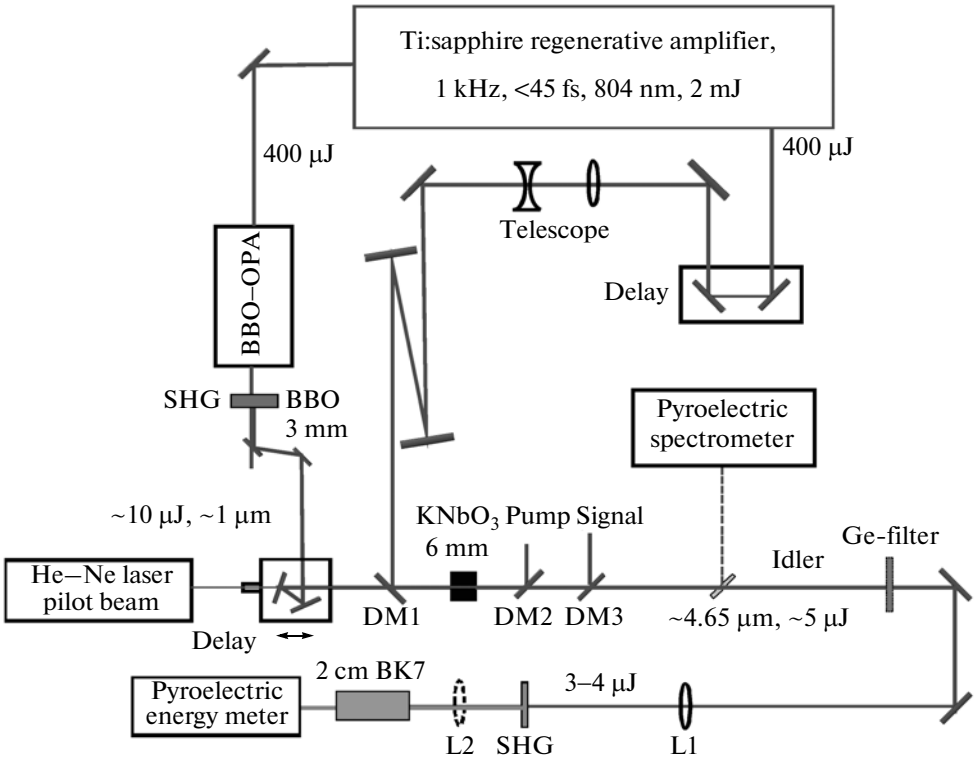

Fig. 6. Experimental setup for relative measurement of the SHG efficiency: DM, dichroic mirrors, L, lenses.

$$d_{22}(GaS_{0.1}Se_{0.9}) = 0.86d_{22}(GaSe), \quad \text{and}$$

$$d_{22}(GaS_{0.4}Se_{0.6}) = 0.76d_{22}(GaSe).$$

Thus, we conclude that the mixed crystals of GaS_xSe_{1-x} possess very high effective nonlinearity, comparable to that of pure GaSe. This contradicts both the underestimations in [1] and the obviously overestimated SHG efficiencies given in [7, 8] without details.

6. DAMAGE THRESHOLD

Laser damage in GaSe and $GaS_{0.4}Se_{0.6}$ was studied at 1064 nm, both with nanosecond pulses and continuous-wave (CW) radiation. The nanosecond pump source was a diode-pumped, electro-optically Q-switched Nd : YAG laser (Innolas GmbH, Germany) optimized for a repetition rate of 100 Hz. According to the specifications, its linewidth amounts to 1 cm^{-1}, $M^2 < 1.5$ and the divergence is <0.5 mrad. The laser generated 100 mJ, 14 ns (FWHM) pulses with an average power of 10 W. The measured energy stability was ±1%. Test plates with a thickness between 0.3 and 1.0 mm were irradiated without focusing the pump beam which had a diameter of $2W_0 = 3.8$ mm. Damage in the form of surface damage and through the plate occurred at 0.48 ± 0.03 J/cm^2 for GaSe and 0.68 ± 0.03 J/cm^2 for $GaS_{0.4}Se_{0.6}$. These values correspond to peak (on-axis) incident fluence. They were averaged for measurements at 5 different points which corresponds to the deviations specified. The peak (on-axis) incident intensities are 34 and 49 MW/cm^2, respectively. It is difficult to compare these values with the literature because normally damage in GaSe was characterized at longer wavelengths [14, 15]: although the value of 35 MW/cm^2, often found in the literature [4] as damage threshold of GaSe at 1064 nm for 10 ns pulses, is consistent with our measurements, it might be a result of erroneous cross citations [24]. Nevertheless, we can conclude that $GaS_{0.4}Se_{0.6}$ possesses higher damage threshold than GaSe, as could be expected from its larger band-gap, although its thermal conductivity could be slightly lower [17]. It should be noted that also gray tracks occurred in $GaS_{0.4}Se_{0.6}$ at a fluence/intensity level roughly corresponding to 80% of the above specified values. Their occurrence seems not related to the surface damage and cracking. Such gray tracks were not observed in GaSe simply because of its deep red color.

The same test plates were irradiated also with a CW Nd : YVO_4 laser operating at 1064 nm. With a 30-mm best shape lens we measured a waist diameter in the focus of $2W_0 = 18$ μm and estimated $M^2 = 1.6$. The maximum power applied, measured after the lens, was 8.5 W which gives a peak intensity of 6.6 MW/cm^2 in the focus. Averaging three measurements at different positions for each sample, we obtained characteristic damage thresholds of 0.6 MW/cm^2 for GaSe and 1 MW/cm^2 for $GaS_{0.4}Se_{0.6}$, at which the front surface was destroyed.

7. TWO-PHOTON ABSORPTION

We investigated the TPA of $GaS_{0.4}Se_{0.6}$ relative to pure GaSe using the picosecond open-aperture (OA) z-scan technique at $\lambda = 1064$ nm. In the OA z-scan experiment, the nonlinear transmission is measured by detecting the intensity-dependent transmission changes when translating the sample along the beam. A 10-Hz passive/active mode-locked Nd : YAG laser (B. M. Industries) with $M^2 = 1.3$ was used. The pulse duration (FWHM) measured by SHG autocorrelation with a BBO crystal, was $\tau = 38$ ps. The output was divided into two beams by a 1 : 5 beam splitter. The beam with higher energy was focused by a 20 cm convex lens on the sample and the other beam served as a reference. The sample was then translated near the focal point. The incident pulse energy in the measurements varied between $\varepsilon_0 = 10.6$ and 11.9 μJ, which corresponds to external (incident) peak on-axis intensity at the focus, $I_0 = 4\sqrt{\ln 2}\varepsilon_0/(\pi^{3/2}W_0^2\tau)$, from 18.3 to 20.5 GW/$cm^2$ for a beam waist of $W_0 = Mw_0 = 30.2$ μm ($w_0 = 26.5$ μm). The pulse energy transmitted through the sample was detected by a large area pyroelectric energy meter.

For Gaussian beams, both in space and time, the normalized transmission $T_N = \varepsilon_{tr}/[e^{-\alpha d}(1-R)^2\varepsilon_0]$ in the OA z-scan measurement can be expressed as a function of the TPA coefficient β. Here ε_{tr} denotes the transmitted energy, R the Fresnel reflection (21–22%), α is the linear absorption (see Section 3), and d is the sample thickness. The expression is simplified assuming that the sample thickness d is much shorter than the Rayleigh length $z_R = \pi w_0^2/\lambda$ [25]:

$$T_N(z) = \frac{2\sqrt{\ln 2/\pi}}{\tau q}\int_{-\infty}^{\infty}\ln(1+qe^{-4\ln 2t^2/\tau^2})dt,$$

where $q = \dfrac{(1-R)\beta I_0 d_{eff}}{1+(z/z_R)^2}$ with the effective length $d_{eff} = (1-e^{-\alpha d})/\alpha$ and z is the translation coordinate. For Gaussian beams, both in space and time, the normalized transmission T_N in the OA z-scan measurement is usually expressed as a simple function of β assuming that the nonlinear losses are small, $(1-R)\beta I_0 d_{eff} \ll 1$ [25]:

$$T_N(z) = 1 - \frac{(1-R)\beta I_0 d_{eff}}{2\sqrt{2}(1+(z/z_R)^2)}.$$

The samples available were a 1.13-mm-thick plate of $GaS_{0.4}Se_{0.6}$ ($d_{eff} = 1.12$ mm) and a 0.9-mm-thick

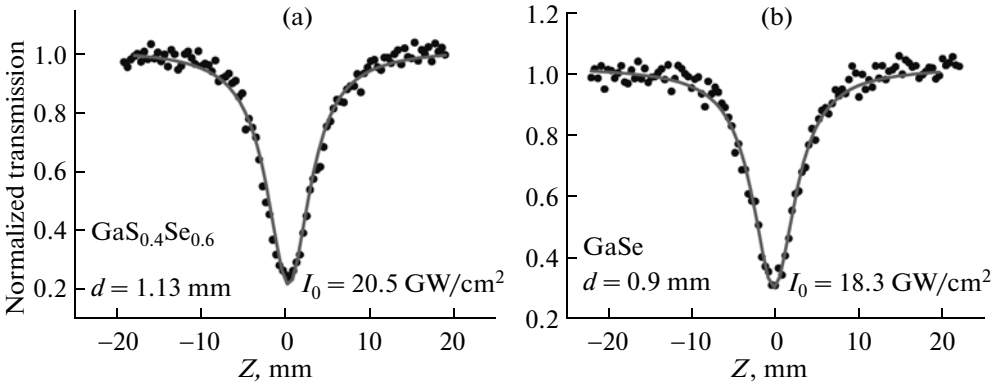

Fig. 7. Open-aperture z-scan signals of $GaS_{0.4}Se_{0.6}$ (a) and GaSe (b) with fit curves. I_0 denotes the peak on-axis intensity incident on the samples.

plate of GaSe ($d_{eff} = 0.88$ mm), both cleaved with faces perpendicular to the c-axis, and thus only the o-polarization could be studied.

In Figs. 7a and 7b, the OA z-scan signals of $GaS_{0.4}Se_{0.6}$ and GaSe are depicted, showing transmission reduction with increasing intensities. The measured data could be well-fitted as a function of the translation coordinate by the last formula. For GaSe the result obtained from Fig. 7b is $\beta = 1.58 \pm 0.04$ cm/GW. This value is very close to the $\beta = 1.4$ cm/GW, measured in [26] for the same geometry, with 10 ps long pulses at a repetition rate of 81 MHz. The value obtained by us for $GaS_{0.4}Se_{0.6}$ was smaller, $\beta = 1.20 \pm 0.03$ cm/GW, which can be attributed to the larger band-gap. Since GaSe and $GaS_{0.4}Se_{0.6}$ are negative crystals, in a practical OPO scheme, the pump will be e-polarized. The two polarizations were compared in [26] for the same GaSe sample by simply rotating it, and thus the ratio of 1.76 for the TPA coefficients can be considered to be very reliable. Assuming a similar ratio for $GaS_{0.4}Se_{0.6}$ one arrives at $\beta \sim 2.1$ cm/GW for the e-polarization. Due to the large birefringence, phase matching angles are, however, small and for generation of idler wavelengths, e.g., around 6.45 μm ($\theta \sim 15°$ for oo-e interaction), the resulting value at the pump wavelength would be $\beta \sim 1.3$ cm/GW. Peak on-axis intensities in the nanosecond (OPO) regime, in any crystal, usually do not exceed 50 MW/cm^2 in order to avoid surface damage (see previous section). Thus the nonlinear losses in $GaS_{0.4}Se_{0.6}$ will be still about two times smaller than the linear losses for a crystal length of 1 cm which seems feasible for OPO having in mind the high effective nonlinearity. The good agreement of the present TPA results for GaSe with other measurements [26] does not mean that the absolute values obtained are reliable. In fact the TPA coefficient is obtained in [26] from transmission measurements where (i) the maximum applied intensity is limited to 120 MW/cm^2, (ii) it remains unclear how the spatial beam profile has been taken into account, and (iii) thermal effects may play a role at 81 MHz repetition rate. Older measurements by the same method as in [26] but with a system very similar to ours (35 ps pulse duration and repetition rate of 10 Hz) gave substantially higher values for the o-polarization in GaSe, 6.3 ± 2.2 cm/GW [27] while the value of 110 cm/GW obtained with 20-ns pulses in a very early experiment [28] is generally accepted to have been affected by poor sample quality, impurities, small dynamic range and free-carrier absorption. Even worse, very recent experimental data of others [29] is just another contribution to the chaos on this issue: with 65 ps pulse duration and 10 Hz repetition rate the authors of [29] give values between $\beta = 32$ and 43.2 cm/GW for the o-polarization in GaSe, which increase with the incident intensity (varied from 49 to 106 MW/cm^2). In fact this means that fitting of the z-scan traces should be impossible and the process observed cannot be described by pure TPA.

On the other hand, our fitting procedure for Fig. 7 obviously violates the assumption for small transmission changes, $(1 - R)\beta I_0 d_{eff} \ll 1$ stated above. We attempted to fit our experimental results using semi-analytical polynomial expressions developed to account for higher values of this parameter [30] but we were unable to obtain satisfactory fits neither with pure TPA or three-photon absorption process nor with combinations of them. It can be speculated that our experimental data in Fig. 7 was recorded at very high intensities (in fact they reached in some cases the damage threshold with 38 ps long pulse) but the signal to noise ratio, related to the poor pulse-to-pulse stability of such kind of laser sources, prevented us from recording reliable z-scans at substantially lower intensity levels.

It is clear that our TPA results in Fig. 7 are not so relevant to OPO operation but rather to travelling-wave schemes like OPG and OPA [31, 32] which require higher pump intensities. At present it can be only speculated if they are affected by different type of nonlinear processes such as free-carrier excitation and absorption at such high intensities [33]. This could

possibly explain the weaker than expected difference in the TPA coefficients that we obtain for GaSe and $GaS_{0.4}Se_{0.6}$ having in mind the fact that GaSe is excited at energies well above half the band-gap.

8. CONCLUSIONS

In conclusion, we demonstrated that the mixed nonlinear crystal $GaS_{0.4}Se_{0.6}$ exhibits promising optical properties including large band-gap, good transparency in the mid-IR, sufficient birefringence for phase-matching, large nonlinear coefficient, large damage threshold and low TPA that make it a good candidate for application in 1064 nm pumped OPOs, OPGs or OPAs. Higher hardness in comparison to GaSe will make it easier for cutting and polishing while the good thermal conductivity could enable operation at high repetition rates. This opens new perspectives for development of such devices operating in the 5–14 μm spectral range which can be directly pumped by Nd:YAG laser systems.

ACKNOWLEDGMENTS

The research leading to these results has received funding from the European Community's Seventh Framework Programme FP7/2007–2011 under grant agreement no. 224042.

REFERENCES

1. K. R. Allakhverdiev, R. I. Guliev, E. Yu. Salaev, V. V. Smirnov, Kvant. Elektron. **9**, 1483 (1982) [Sov. J. Quantum Electron. **12**, 947 (1982)].
2. H. Serizawa, Y. Sasaki, and Y. Nishina, J. Phys. Soc. Jpn. **48**, 490 (1980).
3. C. H. Ho, C. C. Wu, and Z. H. Cheng, J. Cryst. Growth **279**, 321 (2005).
4. K. R. Allakhverdiev, M. Ö. Yetis, S. Özbek, T. K. Baykara, and E. Yu. Salaev, Las. Phys. **19**, 1092 (2009).
5. G. B. Abdullaev, K. R. Allakhverdiev, R. Kh. Nani, E. Yu. Salaev, and M. M. Tagyev, Phys. Status Solidi A **53**, 549 (1979).
6. C. Perez Leon, L. Kador, K. R. Allakhverdiev, T. Baykara, and A. A. Kaya, J. Appl. Phys. **98**, 103103 (2005).
7. S. Das, C. Ghosh, O. G. Voevodina, Yu. M. Andreev, and S. Yu. Sarkisov, Appl. Phys. B **82**, 43 (2006).
8. H.-Z. Zhang, Z.-H. Kang, Y. Jiang, J.-Y. Gao, F.-G. Wu, Z.-S. Feng, Y. M. Andreev, G. V. Lanskii, A. N. Morozov, E. I. Sachkova, and S. Yu. Sarkisov, Opt. Express **16**, 9951 (2008).
9. A. Gouskov, J. Camassel, and L. Gouskov, Prog. Cryst. Growth Charact. **5**, 323 (1982).
10. G. A. Akhundov, N. A. Gasanova, and M. A. Nizametdinova, Phys. Status Solidi B **15**, K109 (1966).
11. C. C. Wu, C. H. Ho, W. T. Shen, Z. H. Cheng, Y. S. Huang, and K. K. Tiong, Mater. Chem. Phys. **88**, 313 (2004).
12. P. G. Rustamov, Z. D. Melnikova, M. G. Safarov, and M. A. Alidzhanov, Izv. Akad. Nauk. SSSR, Neorg. Mater. **1**, 419 (1965) [Inorg. Mater. **1**, 387 (1965)].
13. Z.-S. Feng, Z.-H. Kang, F.-G. Wu, J.-Y. Gao, Y. Jiang, H.-Z. Zhang, Y. M. Andreev, G. V. Lanskii, V. V. Atuchin, and T. A. Gavrilova, Opt. Express **16**, 9978 (2008).
14. D. R. Suhre, N. B. Singh, V. Balakrishna, N. C. Fernelius, and F. K. Hopkins, Opt. Lett. **22**, 775 (1997).
15. N. B. Singh, D. R. Suhre, W. Rosch, R. Meyer, M. Marable, N. C. Fernelius, F. K. Hopkins, D. E. Zelmon, and R. Narayanan, J. Cryst. Growth **198–199**, 588 (1999).
16. V. Petrov, F. Noack, I. Tunchev, P. Schunemann, and K. Zawilski, Proc. SPIE **7197**, 71970M (2009).
17. N. A. Abdullaev, M. A. Aldzhanov, and E. M. Kerimova, Fiz. Tverd. Tela **44**, 213 (2002) [Phys. Solid State **44**, 221 (2002)].
18. P. G. Rustamov, Z. D. Melikova, Ya. N. Nasirov, and M. A. Alidzhanov, Izv. Akad. Nauk SSSR, Neorg. Mater. **5**, 881 (1969) [Inorg. Mater. **5**, 750 (1969)].
19. G. B. Abdullaev, L. A. Kulevskii, A. M. Prokhorov, A. D. Savel'ev, E. Y. Salaev, and V. V. Smirnov, Pis'ma Zh. Eksp. Teor. Fiz. **16**, 130 (1972) [JETP Lett. **16**, 90 (1972)].
20. K. L. Vodopyanov, L. A. Kulevskii, V. G. Voevodin, A. I. Gribenyukov, K. R. Allakhverdiev, and T. A. Kerimov, Opt. Commun. **83**, 322 (1991).
21. K. L. Vodopyanov, J. Opt. Soc. Am. B **10**, 1723 (1993).
22. G. B. Abdullaev, K. R. Allakhverdiev, L. A. Kulevskii, A. M. Prokhorov, E. Y. Salaev, A. D. Savel'ev, and V. V. Smirnov, Kvant. Elektron. **2**, 1228 (1975) [Sov. J. Quantum Electron. **5**, 665 (1975)].
23. E. Takaoka and K. Kato, Jpn. J. Appl. Phys. **38**, 2755 (1999).
24. Ph. Kupecek, E. Batifol, and A. Kuhn, Opt. Commun. **11**, 291 (1974).
25. R. L. Sutherland, *Handbook of Nonlinear Optics*, 2nd ed. (Marcel Dekker, New York, 2003).
26. K. R. Allakhverdiev, T. Baykara, S. Joosten, E. Günay, A. A. Kaya, A. Kulibekov (Gulubayov), A. Seilmeier, and E. Yu. Salaev, Opt. Commun. **261**, 60 (2006).
27. K. R. Allakhverdiev, Solid State Commun. **111**, 253 (1999).
28. F. Adduci, I. M. Catalano, A. Cingolati, and A. Minafra, Phys. Rev. B **15**, 926 (1977).
29. M. Yüksek, A. Elmali, M. Karabulut, and G. M. Mamedov, Appl. Phys. B **98**, 77 (2010).
30. B. Gu, X.-Q. Huang, S.-Q. Tan, M. Wang, and W. Ji, Appl. Phys. B **95**, 375 (2009).
31. T. Dahinten, U. Plödereder, A. Seilmeier, K. L. Vodopyanov, K. R. Allakhverdiev, and Z. A. Ibragimov, IEEE J. Quantum Electron. **29**, 2245 (1993).
32. G. I. Petrov, K. L. Vodopyanov, and V. V. Yakovlev, Opt. Lett. **32**, 515 (2007).
33. H. P. Li, C. H. Kam, Y. L. Lam, and W. Ji, Opt. Commun. **190**, 351 (2001).